Search for New Boson $W_1^{\pm}$ in the Minimal Higgsless Model at the LHC *

Zhen-Xia Zhang[1;1)], Jian-Guo Bian[1], Guo-Ming Chen[1], Ming-Shui Chen[1], Zu-Hao Li[1], Song Liang[1], Xiang-Wei Meng[1], Zhi-Cheng Tang[1], Jun-Quan Tao[1], Zheng Wang[1], Jian Wang[1], Jian Wang[2], Xian-You Wang[4], Hong Xiao[1], Min Yang[1], Jing-Jing Zang[1], Bin Zhang[3], Zhen Zhang[1]

1 (Institute of High Energy Physics, Chinese Academy of Sciences, Beijing 100049, China)
2 (Graduate University, Chinese Academy of Sciences, Beijing 100049, China)
3 (Center for High Energy Physics, Tsinghua University, Beijing 100049, China)
4 (Theoretical Physics Institute, Chongqing University, Chongqing 400044, China)

Abstract The Minimal Higgsless model predicts the existence of new vector gauge boson $W_1^{\pm}$. By the process $PP \rightarrow W_1^{\pm}qq\prime \rightarrow W^{\pm}Z^0qq\prime \rightarrow l^+l^-jjjj$(l=e,$\mu$; j=jets from quark), We study the sensitivity of searching for this possible vector gauge boson in the level of generator events of signal and backgrounds, then give integrated luminosity required to discover 5σ signal as a function of $W_1^{\pm}$ mass. The generator for the signal $PP \rightarrow W_1^{\pm}qq\prime \rightarrow W^{\pm}Z^0qq\prime$ at tree level is developed with the Minimal Higgsless model and then interfaced with PYTHIA for the parton showers and hadronization. The backgrounds are produced with MadGraph and PYTHIA.

Key words Minimal Higgsless model ,$W_1^{\pm}$, discovery potential, integrated liminosity

PACS 12.60.Cn,14.70.Pw

1 Introduction

New spin-1 gauge bosons in Minimal Higgsless Model(MHLM) [1] is one kind of explanation for the mechanism of electroweak symmetry breaking(EWSB). The new bosons play a key role by delaying unitarity violation of longitudinal weak boson scattering up to a higher ultraviolet scale [4, 5] without invoking a fundamental Higgs scalar [6]. The MHLM consists of just three lattice sites(”The Three Site MOdel”) [7], and includes extra nearly degenerate(W_1, Z_1) bosons which are allowed by precision data to be as light as 400GeV [7].

The signature of new boson $W_1^{\pm}$ in the process $pp \rightarrow W^{\pm}Z^0qq\prime \rightarrow \nu 3lqq\prime$ and the process $pp \rightarrow W^{\pm}Z^0Z^0 \rightarrow qq\prime 4l(l = e, \mu)$ were investigated at the parton level, without the initial and final state parton showers and hadronization for the signal and backgrounds and only the background $pp \rightarrow W^{\pm}Z^0qq\prime$ was considered. Assuming $W^{\pm}$ mass within the region of (400, 800) GeV, the integrated luminosity required for 5σ $W_1^{\pm}$ signal detection is from about 7/fb to 30/fb for the first channel, while from about 7.8/fb to 400/fb for the second channel [1]. Considering the initial and final state parton showers and hadronization , even some detector effects including pile-up, particle identity efficiency and so on, this two channels were also researched in references [2, 3].

In this paper, we present the results on the study of $W_1^{\pm}$ production in the process $pp \rightarrow W_1^{\pm}qq\prime \rightarrow W^{\pm}Z^0qq\prime$, $W^{\pm} \rightarrow qq\prime$ and $Z^0 \rightarrow l^+l^-$ by analyzing the fully hadronized events of the signal and backgrounds at the generator level. The generator for the signal of this channel is developed based on the Minimal Higgsless model and interfaced with PYTHIA [8] for the parton showers and parton hadronization. The Feynman diagram for the process $W_1^{\pm}$ production in the process $pp \rightarrow W_1^{\pm}qq\prime \rightarrow W^{\pm}Z^0qq\prime$, $W^{\pm} \rightarrow qq\prime$ and $Z^0 \rightarrow l^+l^-$ is shown in Fig. 1,

Received 10 May 2009
* Supported by National Natural Science Foundation of China (55555555)
1) E-mail: zxzhang@mail.ihep.ac.cn

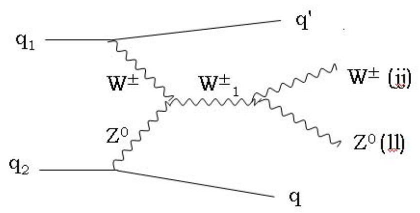

Fig. 1. Feynman diagram for the process $pp \to W^{\pm}Z^0qq\prime \to l^+l^-jjjj$.

in which the intermediate state $W_1^{\pm}$ proceeds throught $W^{\pm}Z^0$ fusion. The typical cross sections (assuming m_{W_1} to be 550GeV) are 48.74 fb and 27.68 fb for $pp \to W_1^{\pm}qq\prime \to W^+Z^0qq\prime \to l^+l^-4q$ and $pp \to W_1^{\pm}qq\prime \to W^-Z^0qq\prime \to l^+l^-4q$ respectively, and $\Gamma_{W_1^{\pm}} \approx 5$GeV according to MHLM.

In this work, we consider the effects of parton showers and hadronization, initial and final state radiation, simulating more backgrounds. This work also considers some detector effects, such as the efficiencies of identifying electrons and muons, the energy resolutions of leptons and jets, and the effects of pile-up events at high LHC luminosities. These improvements add to realism of the study.

2 SIGNAL AND BACKGROUND PRODUCTION

According to the matrix element calculation of the LHC process at a full tree level in the Minimal Higgsless model by the authors of Ref. [1], we obtain the generator for the signal channel $pp \to W_1^{\pm}pp\prime \to W^{\pm}Z^0qq\prime \to l^+l^-4q$. Here the Parton Distribution Function(PDF) CTEQ6L [9] is used. In this work the same pre-selections at the parton level are used as those in Ref. [1]. Jets satisfy transverse momentum $p_{Tj} > 15GeV$ and pseudo-rapidity $|\eta_j| < 4.5$. Leptons satisfy $p_{Tl} > 10GeV$, $|\eta_l| < 2.5$. The weighted parton-level events from the generator are fed into PYTHIA. The initial and final state showers and hadronization are done by PYTHIA.

The cross section after the pre-selection, the number of events produced and the event yields for $100fb^{-1}$ are listed in Table 1, where the event yield is the events number of signal at luminosity of 100 fb^{-1}. The uncertainties of the cross section are discussed in Section IV.

Table 1. Production of signal sample $pp \to W_1^{\pm}pp\prime \to W^{\pm}Z^0qq\prime \to l^+l^-qq\prime qq\prime$. For each mass point, more than 4000 events are produced altogether for W_1^+ and W_1^-. $n_{W_1^+}$ and $n_{W_1^-}$ are different according to their cross sections. The sum of cross sections of W_1^+ and W_1^- is shown with the error statistically estimated from the PDF uncertainty.

$W_1^{\pm}$ mass (GeV)	cross section (fb)	events produced	event yield(100 fb^{-1})
450	126.50± 31.73	4000	12650
500	78.13±14.37	4000	7813
550	76.42±10.20	4000	7642
600	49.07±6.53	4000	4907
650	30.23±7.11	4000	3023
700	28.82±5.87	4000	2882
750	21.80±1.05	4000	2180
800	18.81±1.20	4000	1881

There are two leptons($l = e^{\pm}, \mu^{\pm}$) and four quarks in the signal process. Therefore the contamination to the signal process mainly comes from processes including two leptons and multiple jets in the final state. In view of the final state of the signal process, the backgrounds include: (a) the SM production, $pp \to Z^0 + nj \to l^+l^- + nj$, $1 \leqslant n \leqslant 4$ (b) the SM $t\bar{t}$, $t \to bW^{\pm}$, (c) the SM process $pp \to jjZ^0Z^0 \to jjjjl^+l^-$ with jj=qg, gg, qq, (d) the SM process $pp \to jZ^0Z^0 \to jjjl^+l^-$ with j=q, g, (e) the SM process $pp \to jjW^{\pm}Z^0 \to jjjjl^+l^-$, which is irreducible, (f) the SM process $pp \to W^+W^-Z^0 \to jjjjl^+l^-$, which also is irreducible,(g) the SM process $pp \to jW^{\pm}Z^0 \to jjjl^+l^-$. All the backgrounds channel listed above can make contamination to the signal because of their initial and final radiations, parton showers and their much large cross sections.

In this work, the backgrounds (a)-(g) are simulated using MadGraph [10] interfaced with PYTHIA [11]. The cross sections, the numbers of the events and the event yields of 100 fb^{-1} for the background samples are given in Table 2.

Table 2. Production of backgrounds. j represents a fundamental parton of flavors d, u, s, c, b, t, g.

Process	cross section (fb)	events produced	event yield(100 fb^{-1})
Z^0j	1.248×10^6	10,500,000	124,800,000
Z^0jj	3.955×10^5	4,000,000	39,550,000
Z^0jjj	3.180×10^5	3,717,745	31,800,000
Z^0jjjj	2.324×10^4	228,000	2,324,000
t$\bar{t}$	3.171×10^4	2,923,537	3,171,000
$W^\pm Z^0 jj$	7.847×10^2	499,918	778,470
Z^0Z^0jj	5.365×10^3	408,659	536,500
Z^0Z^0j	7.662×10^3	432,478	766,200
$W^\pm Z^0 j$	8.490×10^2	49,993	84,900
$W^+W^-Z^0$	2.987	9,996	299

3 EVENT SELECTION

The event selection is based on the features of the signal process. There are two leptons with high momentum and four hard partons in the final state. The two leptons come from Z^0 decay. Two of the four partons evolve into hard forward jets and another two partons come from $W^\pm$ also evolving into hard jets. The events are selected if there are two leptons with opposite charge and at least four jets in the final states. At the same time, the leptons are required to satisfy $pt_l > 15GeV$, $|\eta_l| < 2.5$ and jets satisfy $pt_j > 15GeV$, $|\eta_j| < 4.5$. Each jet is reconstructed with cone of $\delta R = \sqrt{\delta\eta^2+\delta\phi^2} = 0.7$ and satisfies $\delta R(j,l) > 0.3$ to suppress fake jets.

The jet reconstruction algorithm is one provided with PYTHIA [11], in which a detector grid is assumed, with the pesudo-rapidity range $|\eta| < \eta_{max}(4.5)$ and the full azimuthal range each divides into 50 equally large bins, giving a rectangular grid; the cell with largest transverse evergy E_T is taken as a jet initiator; a candidate jet is defined to consist of all cells which are within $(\eta-\eta_{initiator})^2+(\phi-\phi_{initiator})^2 < \delta R^2$; the candidate jet is accepted if the summed E_T is above 7 GeV and its all cells are removed from future consideration; the sequence is now repeated within the remaining cell of highest E_T and so on.

Z^0 reconstructed from l^+l^- is required to satisfy

$$|M_{l^+l^-} - 91.18| < 10GeV \tag{1}$$

We select two jets from four good jets to reconstruct $W^\pm$, here the two jets must satisfy $|\eta_j| < 2.0$, transverse momentum over momentum of each jet larger than 0.3, η difference between the two jets less than 1.5 and transverse momentum difference between the two jets less than 250 GeV. The two jets with mass close to $W^\pm$ are used to reconstruct invariant mass of $W^\pm$, which is required to be

$$|M_{W^\pm} - 80.398| < 20GeV \tag{2}$$

because of the worse resolution of jet reconstruction.

The two forward jets are selected from the jets satisfying $|\eta_j| > 1.0$, transverse momentum over momentum of each jet less than 0.3 and η difference between the two jets larger than 3.0 GeV. The invariant mass of the two forward jets is also required to be larger than 400 GeV. We think two jets with largest sum of transverse momentum satisfying above criteria as the two forward jets.

To suppress backgrounds further more, especially the main background $pp \to Z^0 + nj$, we required the maximum transverse momentum of four jets to satisfy:

$$PT_{max}(j) > 100GeV \tag{3}$$

and the sum of transverse momentum of four jets to satisfy:

$$\sum_{i=1}^{4} p_T(j_i) > 300GeV \tag{4}$$

shown in Fig. 2 and Fig. 3 respectively.

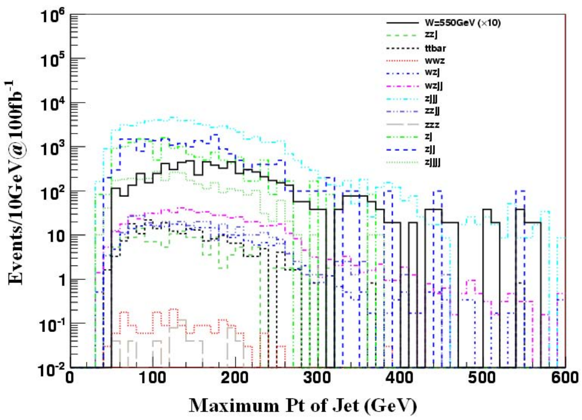

Fig. 2. Maximum transverse momentum of four jets for signal and backgrounds processes.

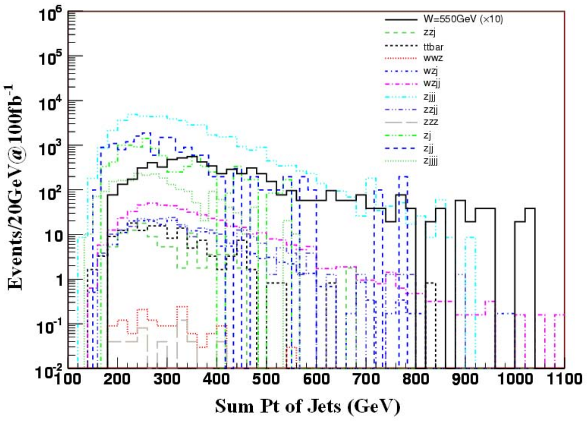

Fig. 3. Sum of transverse momentum of four jets for signal and backgrounds processes.

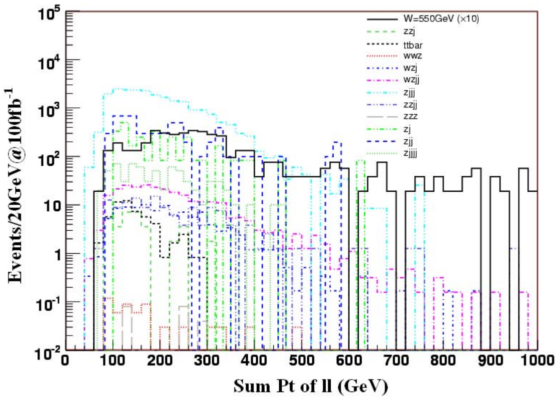

Fig. 4. Sum of transverse momentum of two leptons for signal and backgrounds processes.

In lepton point of view, the sum of transverse momentum of two leptons is required:

$$\sum_{i=1}^{2} p_T(l_i) > 160GeV \tag{5}$$

shown in Fig. 4.

In conclusion, the total numbers and efficiencies for some important cuts for the signal and background samples are shown in Table 3, where $W_1^{\pm}$ mass is 550 GeV.

Table 3. Cut flow. The luminosity is set to be 100 fb^{-1}. The second column is numbers of events, the other columns are remaining efficiencies after each cut. j represents a fundamental parton of flavors d, u, s, c, b, t, g.

Cut	total events	$n_l = 2$	$n_j \geq 4$	$M_{W^\pm} = 80 \pm 20$	forward jets	max$pt_j > 100$	$\Sigma pt_j > 300$	$\Sigma pt_l > 160$
Signal	7,642	0.97	0.89	0.47	0.17	0.15	0.12	0.10
$Z^0 j$	1.24E+08	0.49	0.22	8.49E-03	6.8E-04	2.5E-04	5.8E-05	3.1E-05
$Z^0 jj$	3.96E+07	0.57	0.11	5.8E-02	3.6E-03	1.4E-03	4.2E-04	1.78E-04
$Z^0 jjj$	3.18E+07	0.48	0.22	0.11	9.8E-03	4.5E-03	1.8E-03	7.7E-04
$Z^0 jjjj$	2.32E+06	0.35	0.23	0.13	1.3E-02	4.1E-03	1.1E-03	5.4E-04
$t\bar{t}$	3.17E+06	0.33	2.9E-02	1.8E-02	2.2E-03	9.7E-04	2.9E-04	3.9E-05
jjZ^0Z^0	5.37E+05	8.2E-02	5.2E-02	3.5E-02	3.0E-03	1.5E-03	7.1E-04	3.2E-04
jZ^0Z^0	7.66E+05	8.0E-02	2.9E-02	1.8E-02	1.0E-03	3.8E-04	1.3E-04	5.1E-05
$W^\pm Z^0 jj$	7.79E+05	6.4E-01	5.2E-01	3.4E-01	3.7E-02	2.1E-02	1.0E-02	4.8E-03
$W^+W^-Z^0$	299	6.6E-01	5.1E-01	3.8E-01	2.3E-02	1.2E-02	4.9E-03	2.2E-03
$W^\pm Z^0 j$	8.49E+04	6.1E-01	3.3E-01	2.0E-01	1.7E-02	8.6E-03	3.7E-03	1.8E-03

The spectrum of invariant mass of $W^\pm Z^0$ for signal and background samples are plotted in Fig. 5, after applying these cuts for an intergrated luminosity of 100 fb^{-1}.

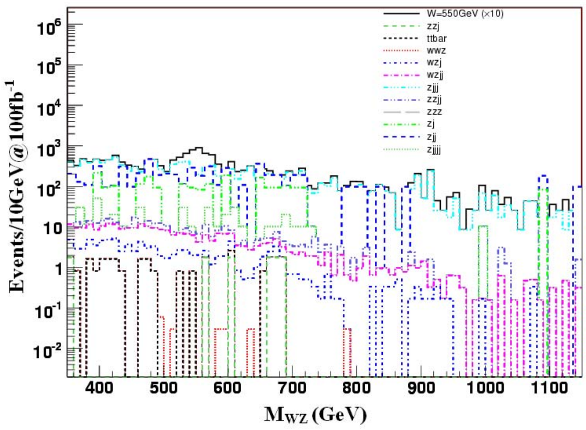

Fig. 5. Distribution of $M_{W^\pm Z^0}$ for signal and backgrounds samples at an integrated lumi-

nosity of $100fb^{-1}$. All histograms are stacked.

The backgrounds Z^0+nj, $W^{\pm}Z^0jj$ and $W^{\pm}Z^0j$ have large contribution to the whole background, while $Z^0Z^0Z^0$, $W^+W^-Z^0$ and Z^0Z^0j are much smaller backgrounds and almost invisible in the spectrum of $W^{\pm}Z^0$. We estimate the expected sensitivity in mass region of $M_{Z^0W^{\pm}} = M_{W_1^{\pm}} \pm 50GeV$ using the formula

$$S=\sqrt{2ln(Q)}, Q=(1+N_s/N_b)^{N_s+N_b}exp(-N_s) \quad (6)$$

here N_s and N_b are events number of signal and whole background respectively in each mass region. The expected sensitivity is $3.37\pm0.71\sigma$, which corresponds to 5.0σ for the integrated luminosity of $219.71\pm92.69fb^{-1}$.

The same procedure with the same selection creteria is applied to the signal process with $M_{W_1^{\pm}}$ =450, 500, 550, 600, 650, 700, 750, 800 GeV. The remaining events, the significance for $100fb^{-1}$ and the intergrated luminosity for 5σ detection are shown in Table 4, where the errors represent the effect of systematics and statistics.

Table 4. The number of events(in the mass window $M_{Z^0W^{\pm}} = M_{W_1^{\pm}} \pm 50GeV$), the significance with the integrated luminosity of $100fb^{-1}$ and the integrated luminosity for 5σ signal detection.

$m_{W_1^{\pm}}(GeV)$	number of signal (error)	number of bg (error)	σ for 100 fb^{-1} (with sys. error)	lumi(fb^{-1}) for 5σ (with sys. error)
450	230 (27.74%)	8556 (23.24%)	2.52 (0.75)	393.65 (235.56)
500	269 (21.87%)	7803 (23.24%)	3.03 (0.75)	271.86 (133.73)
550	274 (17.83%)	6488 (23.24%)	3.37 (0.71)	219.71 (92.69)
600	113 (17.80%)	5596 (23.24%)	1.50 (0.32)	1108.24 (469.13)
650	79 (26.30%)	4504 (23.24%)	1.17 (0.34)	1814.72 (1040.04)
700	66 (23.58%)	3431 (23.24%)	1.12 (0.29)	1981.71 (1037.95)
750	52 (12.77%)	2191 (23.24%)	1.10 (0.19)	2041.67 (701.02)
800	43 (13.40%)	1478 (23.24%)	1.11 (0.20)	2017.66 (710.86)

4 SYSTEMATIC UNCERTAINTIES

The systematic errors we consider here mainly include:

1)The cross section uncertainty for the signal process includes the statistical error and the difference between PDFs CTEQ6L1 [12] and CTEQ6M140 [13] listed in Table 1. The uncertainty of cross sections for backgrounds is assumed to be 20% [14].

2)Due to initial and final state radiation modeling, parton shower and pile-up, the uncertainty is estimated to be 10% [14].

3)The relative uncertainty for lepton identification and reconstruction is assumed 2% [14]. In this process, there are two leptons and the corresponding systematic error for event yield is 4% [3].

4)In the same method as above, the uncertainty for event yield is 0.5% due to 10% uncertainty of lepton p_T resolution [3, 14].

5)The uncertainty is estimated to be 10% for jet energy resolution and 7% for jet energy scale [14]. For the final state with two jets, they bring the uncertainty 2% and 1% respectively for the event yield [3]. So we can obtain 4% and 2% systematic error respectively to this two sources in our process with four jets in the final state.

6)In reconstruction of jet, 5% of them can be identified to be lepton by mistake [14]. In this process, jets faking leptons bring 2% uncertainty to event yield in case of four jets [3].

All the uncertainties of events yields are listed in Table 5 for signal processes and backgrounds samples.

Table 5. The uncertainties for event yields common to signal and background samples.

Source	Uncertainty
parton shower, plie-up	10%
lepton p_T resolution	0.5%
lepton ID efficiency	4%
jet energy scale	4%
jet energy resolution	2%
jets faking leptons	2%

In conclusion, the total uncertainty for remaining event numbers of backgrounds is 18.44% shown in Table 4. Considering the uncertainty of cross sections of signal samples, the total uncertainty for signal samples of every energy region are also shown in Table 4, which contains the errors in Table 5 and the uncertainty of generation cross sections for each sample with different energy region respectively.

5 SUMMARY

We studied discovery potential of a new charged boson $W_1^{\pm}$ in the process $pp \rightarrow W_1^{\pm} jj \rightarrow W^{\pm} Z^0 jj \rightarrow l^+ l^- jjjj (l = e, \mu)$ based on hadronized events with the initial and final state parton showers at the generator level. The signal generator is developed with the Minimal Higgsless model. As much as possible backgrounds sample are taken into account in background study. Detector effects are also simulated. Theoretical and experimental uncertainties are estimated. The integrated luminosity for 5σ signal detection is present. By this process, the new vector boson $W_1^{\pm}$ may be found in LHC experiments if the mass value is less than 600 GeV, given that it really exists according to the theoretical prediction.

References

1 B. Zhang, Y. Kuang *et al.*, Phys. Rev. D **78**, 031701(2008).

2 Jian-Guo Bian (*et al.*), *Discovery potential of new boson in the Minimal Higgsless model at LHC.(To be published in Nuclear Physics B.)*

3 *Ming-Shui Chen et al., J. Phys. G: Nucl. Part. Phys. 36 (2009) 075004.*

4 *R. S. Chivukula, D. A. Dicus, and H. J. He, Phys. Lett. B* **525**, *175(2002); R. S. Chivulula and H. J. He, Phy. Lett. B* **532**, *121(2002); R. S. Chivukula, D. A. Dicus, H. J. He, and S. Nandi, Phys. Lett. B* **562**, *109(2003).*

5 *H. J. He, Int. J. Mod, Phys. A* **20**, *3362(2005).*

6 *P. W. Higgs. Phys. Lett.* **12**, *132(1964).*

7 *R. S. Chivukula, B. Coleppa, S. Di Chiara, E. H. Simmons, H. J. He, M. Kurachi, and M. Tanabashi, Phys. Rev. D* **74**, *075011(2006).*

8 *hep-ph/0308153, T. Sjostrand, L. Lonnblad, S. Mrenna and P. S. Kands.*

9 *J. Pumplin et al., JHEP* **0207** *012(2002) and D. Stump et al., JHEP* **0310** *046(2003).*

10 *J.Pumplin et al., JHEP* **028A** *09 (2009).*

11 *T.Sjöstrand et al., Comput. Phys. Commun.* **135**, *238(2001).*

12 *J. Pumplin et al., JHEP* **0207** *012 (2002) and D.Stump et al., JHEP* **0310** *046 (2003).*

13 *H. L. Lai et al., Eur. Phys. J.* **12**, *375 (2000).*

14 *The ATLAS Collaboration, $Detector and Physics Performance-Technical Design Reports$,* **CERN/LHCC/99-15**, *vol.1.*